Available online at www.sciencedirect.com
ScienceDirect
Journal of Colloid and Interface Science 303 (2006) 404–414
JOURNAL OF Colloid and Interface Science
www.elsevier.com/locate/jcis

Structural and redox properties of mitochondrial cytochrome *c* co-sorbed with phosphate on hematite (α-Fe_2O_3) surfaces

Nidhi Khare, Carrick M. Eggleston *, David M. Lovelace, Steven W. Boese

Department of Geology and Geophysics, University of Wyoming, Laramie, WY 82071, USA

Received 28 February 2006; accepted 27 July 2006

Available online 1 August 2006

Abstract

The interaction of metalloproteins with oxides has implications not only for bioanalytical systems and biosensors but also in the areas of biomimetic photovoltaic devices, bioremediation, and bacterial metal reduction. Here, we investigate mitochondrial ferricytochrome *c* (Cyt *c*) co-sorption with 0.01 and 0.1 M phosphate on hematite (α-Fe_2O_3) surfaces as a function of pH (2–11). Although Cyt *c* sorption to hematite in the presence of phosphate is consistent with electrostatic attraction, other forces act upon Cyt *c* as well. The occurrence of multilayer adsorption, and our AFM observations, suggest that Cyt *c* aggregates as the pH approaches the Cyt *c* isoelectric point. In solution, methionine coordination of heme Fe occurs only between pH 3 and 7, but in the presence of phosphate this coordination is retained up to pH 10. Electrochemical evidence for the presence of native Cyt *c* occurs down to pH 3 and up to pH 10 in the absence of phosphate, and this range is extended to pH 2 and 11 in the presence of phosphate. Cyt *c* that initially adsorbs to a hematite surface may undergo conformation change and coat the surface with unfolded protein such that subsequently adsorbing protein is more likely to retain the native conformational state. AFM provides evidence for rapid sorption kinetics for Cyt *c* co-sorbed with 0.01 or 0.1 M phosphate. Cyt *c* co-sorbed with 0.01 M phosphate appears to unfold on the surface of hematite while Cyt *c* co-sorbed with 0.1 M phosphate possibly retains native conformation due to aggregation.

Keywords: Adsorption; Phosphate; Cytochrome *c*; Conformation change; Hematite; Oxide

1. Introduction

The interaction of cytochrome *c* with oxide electrodes has been studied for some time [1] because it is important as a baseline for understanding bacterial electron transfer [2], redox catalysis for dehalogenation of halocarbon contaminants [3–5], development of biosensors and bioanalytical systems [6–8], bioremediation [9–13] and emerging photovoltaic applications [14,15]. For new biosensors, direct electrochemistry of redox proteins on electrode surfaces [16] requires that adsorbed proteins retain redox activity. For example, organic ions (4,4′-bipyridine is an early example [17]) have been used to prevent denaturation of adsorbed cytochrome *c* and to orient the heme group toward the surface to promote electron transfer [18]. Boussad et al. [19] showed that phosphate can serve in a similar role for cytochrome *c* sorbed on graphite electrodes. Here, we investigate the co-sorption of mitochondrial cytochrome *c* (Cyt *c*) with phosphate on hematite (α-Fe_2O_3) surfaces, and the effect of phosphate upon Cyt *c* properties while in the sorbed state, using a combination of wet chemical techniques, optical spectroscopy, atomic force microscopy, and cyclic voltammetry. Hematite was chosen because it is the only ferric oxide that occurs, or can be made, sufficiently conductive (through n-type doping) for use as an electrode [20–22].

A study of Cyt *c* co-sorbed with phosphate on hematite surfaces may also have implications for the heterogeneous self assembly of lipids and integral membrane proteins on mineral surfaces, a process thought to possibly have served as a step in the origin of life [23]. In addition, *c*-type cytochromes isolated from the outer membrane of *Shewenella oneidensis* MR-1 (such as OmcA and MtrC) have been implicated in respiratory electron transfer to oxide surfaces [24–27]. Cyt *c*, because it has been studied since the 1920s [28–32] and shares some properties with these outer membrane cytochromes in some conformations (e.g., [33]), makes a useful comparative baseline for work

* Corresponding author. Fax: +1 307 766 6679.
E-mail address: carrick@uwyo.edu (C.M. Eggleston).

0021-9797/$ – see front matter
doi:10.1016/j.jcis.2006.07.070

with the outer membrane cytochromes. Cyt *c* is a peripheral c-type cytochrome responsible for transferring electrons from the mitochondrial bc_1 protein complex to cytochrome $a-a_3$ complex, and its complexation-induced conformation change allows it to perform its known functions [34]. Because phosphate is relatively common in nature and is known to affect Cyt *c* properties on other surfaces [19], its co-sorption with and effect upon Cyt *c* on hematite is a useful step in understanding the interaction between cytochromes and natural oxide surfaces more generally.

In a previous paper [35], we characterized the adsorption of Cyt *c* on hematite in the absence of phosphate. Our results indicated that sorption of Cyt *c* to hematite is dominated by electrostatic attraction that should orient Cyt *c* molecules with the heme center relatively close to the hematite surface. Direct electrochemistry of Cyt *c* using natural hematite single-crystal electrodes was observed. Although we found no direct evidence of major conformation change upon sorption, the unusually high sorption density, red-shifts in Soret band absorption by Cyt *c* in supernatant solutions, and a slightly negative reduction potential exhibited by Cyt *c* interacting with hematite electrodes as compared to native Cyt *c* are all evidence of possible conformation change upon adsorption. We therefore also studied phosphate co-sorption with Cyt *c* because phosphate may have an influence upon the conformational stability of sorbed Cyt *c*. Our results suggest that Cyt *c* undergoes a conformation change upon interaction with iron oxide, even at pH values for which it remains in the native state in solution.

2. Materials and methods

2.1. Hematite

Hematite was synthesized by the method of Sugimoto et al. [36], and its structure was confirmed using powder XRD. SEM images showed hematite platelets of roughly 1 μm diameter dominated by (001) surfaces. Previous batches of hematite made with this method yielded powders with a N_2 BET surface area 4.76 $m^2\,g^{-1}$. Hematite was washed three times with 1 M KCl solution and further washed with 0.01 M KCl to obtain a 0.01 M KCl background electrolyte [37] and stored as stock aqueous suspension of 94.1 g hematite kg^{-1} (measured) solids concentration.

2.2. Cyt c

Cyt *c* from horse heart was obtained from Sigma and used without further purification. Cyt *c* is a 12.4 kDa globular protein (104 amino acid residues and a covalently attached heme group; PDB ID: 1hrc) with a diameter of about 3.4 nm. Cyt *c* contains 19 lysine residues, of which Lys 13, 27, 72 and 79 are grouped around the heme edge of the molecule. The high lysine content makes Cyt *c* a basic protein, with an isoelectric point of ∼10 [31,38]. The distribution of the lysine residues is not homogeneous, imparting to Cyt *c* dipole moments of 308 and 325 D for the reduced and oxidized forms, respectively [39,40]. This charge distribution is a key factor in the orientation and docking of the cytochrome with cytochrome c oxidase and reductase [41,42] as well as in controlling the redox potentials of the protein (e.g., [41]). The Fe in the heme group is axially coordinated by histidine 18 and methionine 80 in the native state, maintaining the Fe in the low-spin state. The bond between the sulfur of methionine 80 and the Fe of the heme can be disrupted at low and high pH, or at elevated temperature. In some unfolded states, methionine 80 is replaced by histidine 33 [33] to make a his–his coordinated cytochrome, similar to the heme coordination found in cytochromes from iron-reducing and sulfate-reducing bacteria (e.g., [24,42]). The breaking of the Fe–S bond is a mechanism for switching to the high spin state, and allows a portion of the polypeptide chain (from residue 78 to residue 90) to move away from the heme, allowing for ligand replacement. The positively charged edge of Cyt *c* is optimized for electrostatic interaction with negatively charge portions of physiologic partners, and apparently allows interaction with negatively charged electrode surfaces as well. A variety of conformational states have been identified using XANES spectroscopy [43].

2.3. Aqueous experiments

Sorption experiments with hematite suspensions have been described in Khare et al. [35,37]. All samples had a suspended solids concentration of 1.50 g kg^{-1}, constant ionic strength of 0.01 M KCl and total sample mass of 30 ± 0.01 g. Aqueous solutions for sorption experiments (KCl, HCl, KOH all at 0.01 M and Cyt *c* at 0.0001 M) were prepared using analytical grade reagents and degassed (heated and N_2 purged) deionized water. Briefly, 5000 μL of 0.0001 M Cyt *c* solution in 0.01 or 0.1 M phosphate was slowly added to each vigorously stirred sample containing 0.478 g hematite in 0.01 M KCl. The pH was adjusted from 1.7 to 12.3 using a 0.1 M HCl or 0.1 M KOH solution in addition to 0.01 M HCl or 0.01 M KOH for adjusting pH to 1.7, 2.0, or 11.0, 12.0, 12.3, respectively. Each sample was brought to its final mass of 30 g. The sample headspace was flushed with N_2 gas. After equilibration, samples were centrifuged at $\sim 6000g$ for 10 min and the supernatant solutions were decanted and filtered using 0.2-μm polycarbonate membranes. Dissolved Cyt *c* was measured in the supernatant solutions using the Soret band absorption at 408 nm. Sorbed Cyt *c* was determined as the difference between total added Cyt *c* and Cyt *c* measured in supernatants.

2.4. Model calculations

The pH-dependent charge of Cyt *c*, of the surface of hematite in the presence and absence of phosphate, and of Cyt *c* binding to phosphate were calculated as described previously [35] using MICROQL and available surface ionization and phosphate binding constants [44,45]. A Hamaker constant of 10^{-20} J with a simple block model [46,47] was used for approximating van der Waals attraction. Electrostatic forces between a hematite surface and Cyt *c* were estimated using a point charge corresponding to the charge of an Cyt *c* molecule positioned 1.0 nm

above a 100 nm^2 area. Cyt *c* and hematite surface charge density for each pH were used in the pH-dependent force calculation; a dielectric constant of 10 was used as an approximation for structured interfacial water.

2.5. Conformation of Cyt c using optical absorption spectroscopy

Light absorption by heme proteins in the visible region (i.e., the Soret band) depends on Fe ligation in the heme and gives an indication of changes in conformational state of the heme macrocycle. However, because conformational changes ranging from relaxation of the heme pocket to a complete disruption of secondary and tertiary structure could account for the altered heme environment, optical absorption is not structurally specific [48].

2.6. AFM imaging of Cyt c sorbed to hematite surfaces

Cyt *c*, and Cyt *c* co-sorbed with 0.01 M KH_2PO_4 or 0.1 M NH_4PO_4, were imaged on hematite (001) surfaces using a Digital Instruments Nanoscope IIIa operating in both contact and AC imaging modes with Al-coated etched silicon tips/cantilevers.

2.7. Electrochemical characterization of Cyt c using hematite electrodes

A CH Instruments 900 bipotentiostat was used for voltammetry. Cyclic voltammograms (CV) were obtained using a ~25 mm^2 hematite crystal working electrode with electron donor impurity (Sn and Ti) concentration of 2×10^{-3} at% (7.5×10^{17} donors cm^{-3}; [35]). A Pt wire counter electrode and Ag/AgCl reference electrode (made from an oxidized Ag wire in a glass capillary tube filled with 3 M KCl with a platinum leak plug) were used. The Ag/AgCl reference tested 25 ± 1 mV positive of a commercial Ag/AgCl reference electrode in each check. The electrochemical cell was stirred and purged of O_2 using ultra high purity N_2 gas. Control CV experiments were conducted with a hematite electrode in 10 mM KCl (no Cyt *c* or phosphate) over the entire pH range studied here. At pH 2 a faint redox wave with midpoint potential of +450 mV occurred, and at high pH (10 and 11) an oxidation wave occurred at about −300 mV without a clear cathodic reduction peak. These waves are of unknown origin, although we suspect that the most negative potentials lead to incipient alteration of the hematite electrode that results in currents that should not be attributed to electron exchange with Cyt *c*. It should also be noted that at low pH, reduction of H^+ to H_2 may lead to higher cathodic currents and higher interfacial pH than would otherwise be the case. The peaks we observe and attribute to Cyt *c* redox reactions are superimposed on this background.

Because of the need to dip the natural crystal electrodes into the electrolyte solution, sample areas and thus currents are not directly comparable from experiment to experiment, and we therefore focus on the potentials of redox waves rather than currents. CV scans at 20, 50 100, 200, 10, and then a 20 mV s^{-1} repeat (in that order) were collected between 0.6 and −0.6 V vs Ag/AgCl in the presence and absence of phosphate.

3. Results and discussion

3.1. Cyt c sorption to hematite surfaces

Cyt *c* sorption to hematite, in the absence of phosphate and co-sorbed with 0.01 M or 0.1 M phosphate, is shown in Fig. 1. Sorption of Cyt *c* with phosphate shows similar pH dependence as Cyt *c* sorbed without phosphate. Peak sorption occurs in a narrow pH range between pH 8 and 10, with a slight broadening of the adsorption peak on the low-pH side in the presence of phosphate. However, significant adsorption occurs down to about pH 4. The horizontal dashed line in Fig. 1 indicates the amount of protein expected to adsorb to form a hexagonally close-packed monolayer of Cyt *c* in the native state. Peak adsorption, therefore, requires multilayer adsorption (6.3 monolayers). The coverage calculations assume, however, that the protein retains native conformation upon adsorption, and ignore the possibility of protein aggregation. Below, we discuss evidence that neither of these conditions are met.

Residue modification studies have shown that only lysine residues flanking the heme edge are significantly involved in Cyt *c* interaction with negatively charged redox partners and hexametaphosphate anions [49]. Three phosphate binding sites on Cyt *c* have been identified: One is near Lys87 with a dissociation constant of 2×10^{-4} M, another is close to Lys25–His26–Lys27 with a dissociation constant $> 2 \times 10^{-3}$ M, and a third may be close to Lys13 [45]. These binding sites flank the

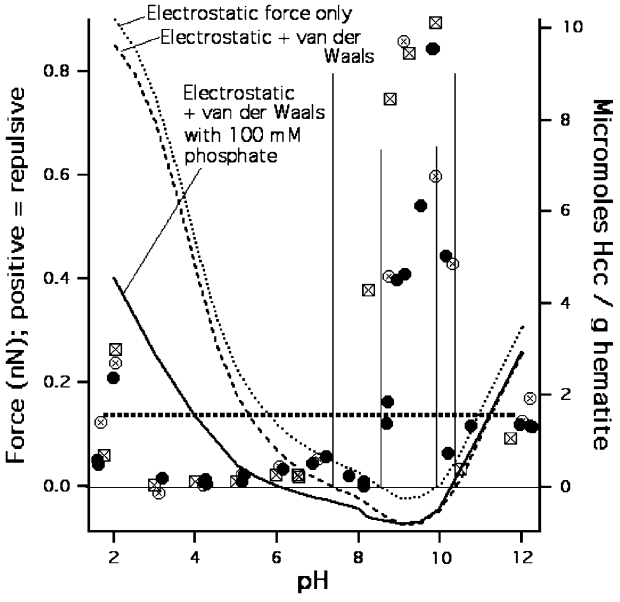

Fig. 1. Sorption of Cyt *c* on hematite in the absence of phosphate (filled circles, right axis), in the presence of 0.01 M (crossed circles, right axis) and 0.1 M (crossed squares, right axis) phosphate as a function of pH. Dotted, dashed, and solid black lines give overall repulsive (positive) or attractive (negative) forces between hematite and Cyt *c* (details about force calculation are found in the main text). The horizontal gray line gives the amount of sorption corresponding to one monolayer of Cyt *c* in hexagonal close packing.

heme groove of Cyt *c*, where bound phosphate would counter the positive charge of lysines.

In addition, phosphate binds to hematite and affects its surface charge. Phosphate adsorption shifts the point of zero charge of hematite, and the isoelectric point of Cyt *c*, toward lower pH. This suggests that, as pH rises, the onset and peak of Cyt *c* adsorption should take place at lower pH in the presence of phosphate than in its absence. The pH of maximum Cyt *c* sorption shifts from pH 9.8 in the absence of phosphate to pH 9.1 in the presence of 0.01 M phosphate (Fig. 1), qualitatively consistent with this expectation. The forces of repulsion or attraction calculated on the basis of phosphate binding made use of the binding constants given above, as well as phosphate adsorption data derived from a study of phosphate sorption to our hematite particles (data not shown). The calculated forces, including electrostatic forces in the presence of phosphate and van der Waals forces, suggest that attractive forces between Cyt *c* and hematite occur mainly on the low pH side of the sorption peak. We only observe enhanced Cyt *c* binding in the presence of phosphate in the pH 8–9 range, and not also in the pH 6–8 range as predicted by calculation (Fig. 1). The phosphate binding constants used in our calculation come from studies done near pH 8, and thus the binding constants likely do not apply to lower pH values, leading to some discrepancy between our calculated forces of attraction and our data between pH 6 and 8.

We conclude that the presence of phosphate does not fundamentally alter the basic electrostatic binding mechanism. The presence of phosphate causes relatively subtle shifts that are consistent with the predicted electrostatic effects of phosphate binding to both Cyt *c* and the hematite surface. Our results are consistent with previous findings on Cyt *c* binding to electrode/electrolyte interfaces [50], negatively charged macromolecular systems [51] and negatively charged redox partners [39] in which interactions are found to be primarily electrostatic. However, multilayer adsorption and other observations presented below suggest that other processes and forces influence Cyt *c* adsorption (and influence properties while in the adsorbed state) as well.

3.2. Conformation of dissolved Cyt c

Cyt *c* changes conformation as a function of pH [43]. Conformation changes, and specifically changes in the immediate coordination environment of Fe in the heme macrocycle, are reflected in the optical absorption spectrum and are interpreted in terms of the simplified molecular orbital diagram shown in Fig. 2 [45]. For example, due to strong configuration interaction between both transitions 1 and 2 from π to π^* orbitals of the porphyrin ligand (Fig. 2), the absorption spectrum displays one strong absorption band at ∼400 nm (referred to as the Soret band) and a weaker absorption band (Q band) between 520 and 550 nm. The weak charge transfer band due to electronic transitions 8, 9, or 10 (Fig. 2) at 695 nm is diagnostic of the Fe–S (of methionine) ligation [52].

Native Cyt *c* heme Fe is axially ligated to his18 and met80 to yield a six coordinated low spin form (6cLS) [53]. In the

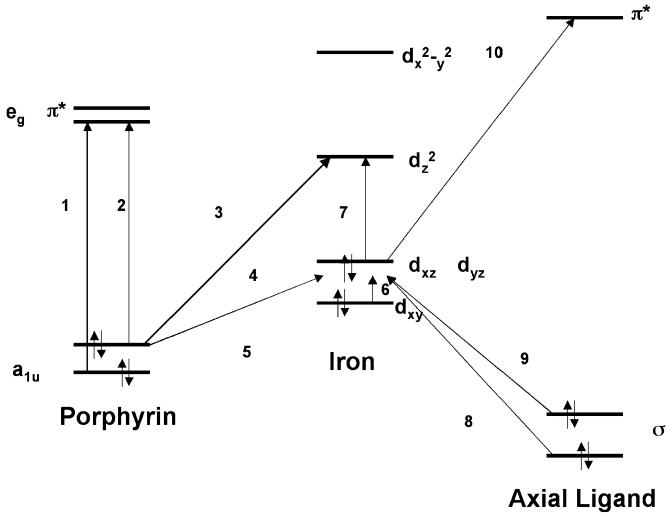

Fig. 2. A simplified molecular orbital diagram showing the transitions responsible for the Soret band (1 and 2), Q bands (1 and 2), and the charge transfer band (3, 4, 8, 9, and 10) based on Pettigrew and Moore [45].

oxidized form, Cyt *c* exhibits the characteristic Soret band at 409 nm, 5 to 10 times lower intensity Q band at 528 nm both originating from the porphyrin chromophore and a weak charge transfer band at 695 nm [34]. Between pH 3 and 7, Cyt *c* in solution is in the native state with intact Fe–S ligation, showing the band positions discussed above (Fig. 3; see also [35]). Between pH 8 and 11, the Soret band blue-shifts to 406 nm, the Q band splits into two bands (one at 520 nm and the other at 548 nm) [35] akin to those observed in reduced Cyt *c* (e.g., [33,54]). A weak shoulder at 582 nm is also observed [35]. The blue-shifted Soret bands indicate a widening of the HOMO (π of porphyrin) and LUMO (π^* of porphyrin) gap and thus a stabilization of the porphyrin macrocycle. In addition, the absence of the charge transfer band at 695 nm (Fig. 3c) indicates that the Fe ligation by methionine is lost. At pH 12, a broadened Q band at 530 nm is seen, with little further change in the Soret band [35]. Lowering the pH below 3 protonates acidic residues and leads to electrostatic destabilization [53] of the polypeptide and hence to changes in the tertiary structure of the protein. The conformation change below pH 3 in the heme macrocycle (alone) is reflected in blue-shifted Soret and Q bands at 394 and 495 nm, respectively, and a new band at 620 nm [35], all indicative of a 6cHS species [34] associated with more negative reduction potentials (see below).

Optical absorption spectra for Cyt *c* in 0.01 M phosphate ions show similar pH dependence as in the absence of phosphate, i.e., native conformation of the heme macrocycle between pH 3 and 7 and changes in the conformation of the heme macrocycle at pH > 7 (Figs. 3a and 3b). At pH 10, the absorption band at 695 nm appears in the presence of phosphate ions but is absent from phosphate-free Cyt *c* solutions, suggesting that phosphate stabilizes Fe–S ligation up to pH 10 (Fig. 3c). In addition, the Q band is similar to native Cyt *c*, rather than split in the absence of phosphate (Fig. 3b). These results suggest that phosphate can counteract pH-dependent conformation change affecting the heme macrocycle of Cyt *c* between pH 7 and 10.

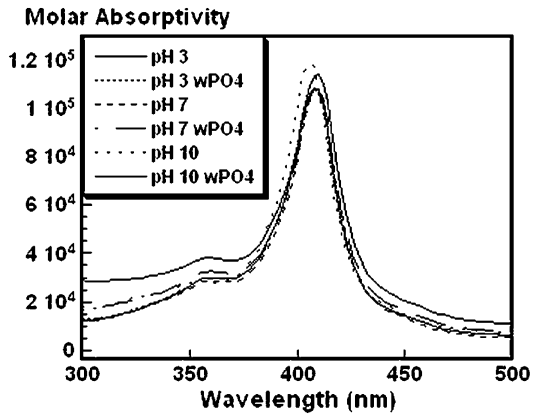

(a)

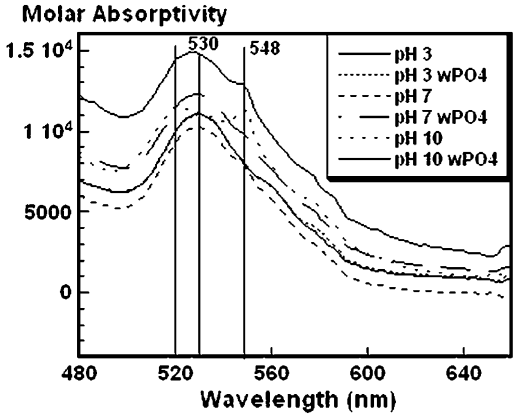

(b)

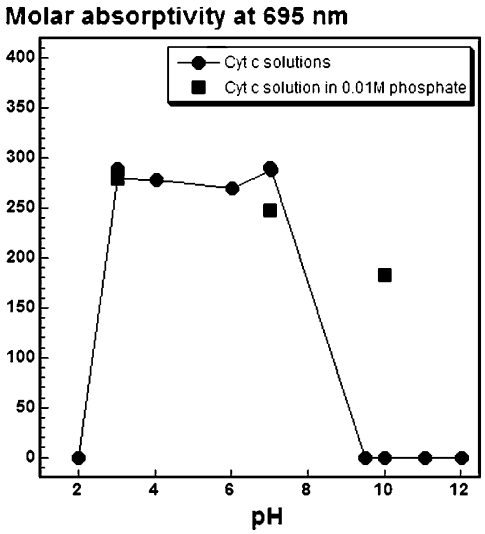

(c)

Fig. 3. (a) and (b): Normalized UV–vis spectra for molar absorptivity of Cyt *c* dissolved in 0.01 M phosphate show essentially no difference with phosphate concentration in the pH range 3–10: (a) Soret band; (b) Q bands; (c) absorbance at 695 nm as a function of pH, with and without 0.01 M phosphate.

3.3. Electrochemical evidence of conformation change

The flatband potential (V_{fb}) of n-type hematite varies with doping level [55], but occurs at about −300 mV vs Ag/AgCl at pH 7 (measured for our natural hematite electrodes using both Mott–Schottky and photocurrent onset techniques) and exhibits Nernstian behavior at high ionic strength [55]. Potentials positive of V_{fb} lead to a space charge layer (Schottky barrier) depleted in charge carrier electrons, inhibiting (or "blocking") electron exchange with solution–phase redox couples (and leading to the very low currents we observe). At pH 2 and 3, V_{fb} is about 0 and −60 mV, respectively. At potentials negative of V_{fb}, there is no blocking space charge layer. Thus, there is greater cathodic current at pH 2 and 3 than at higher pH because V_{fb} is within the CV potential scan range. Because the solution is purged of oxygen, the cathodic current at low pH is probably due to H^+ reduction to H_2 at the most negative potentials (although incipient reduction of the hematite electrode cannot be ruled out). The entire CV flattens out at high pH because V_{fb} moves to very negative values and a blocking layer exists over the entire CV scan range (Fig. 4). Note, however, that the existence of a "blocking layer" does not block all electron exchange but rather simply reduces it in comparison with the unblocked state.

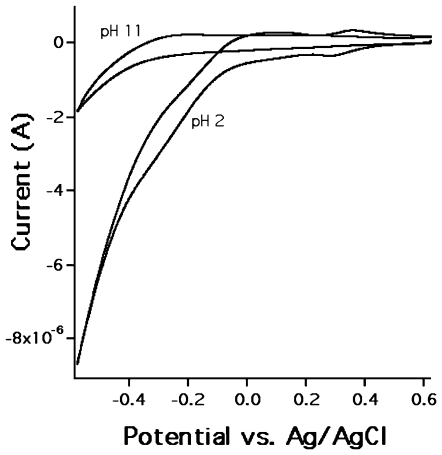

Fig. 4. Example cyclic voltammograms (current vs potential) of Cyt *c* solution at pH 2 and 11 using a hematite working electrode, Pt counter electrode and an Ag/AgCl reference electrode (both for 20 mV s^{-1} scan rate).

Fig. 5 shows a CV (and derivative of the cathodic scan) taken without phosphate at pH 3. This CV shows all three commonly observed redox potentials exhibited by Cyt *c*. Redox potentials are directly related to the conformational state of the protein [50,56,57]. The redox peaks with midpoint potential at about +300 mV is more oxidizing than that of the native protein; it has been observed by others [56] and may indicate a third conformational state of the cytochrome in which the heme is axially coordinated by histidine and lysine, a feature known for other *c*-type cytochromes (e.g., [58]) and reasonably likely given the number of lysine residues in Cyt *c* [29]. The native conformational state occurs at about +50 mV (which compares well with +70 mV [56] for native Cyt *c*), and a more reducing conformational state occurs at about −335 mV that is characteristic of histidine–histidine or histidine–water axial heme coordination [33,56,59]. The existence of several conformational states at low pH may reflect dynamic equilibrium between conformational states. The current associated with each conformation state varied as a function of pH, and some states were not observed for some conditions. From data such as that presented in Fig. 5, reduction peak positions are plotted as a function of

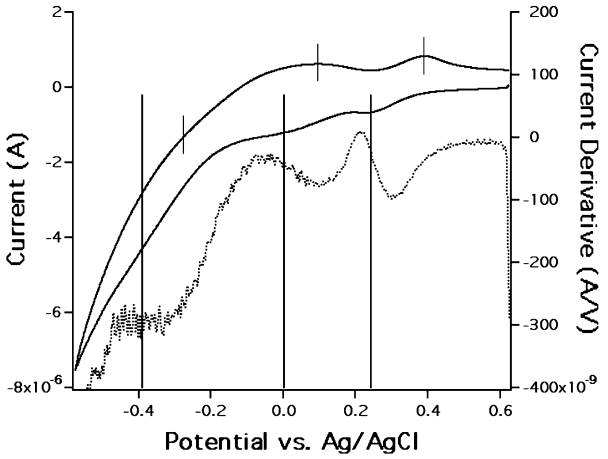

Fig. 5. CV (20 mV s^{-1} scan rate) of Cyt *c* at pH 3 (solid lines) using a hematite electrode (same setup as Fig. 4); a derivative trace of the cathodic scan is included (dotted line). This voltammogram is chosen because it clearly shows all three commonly observed Cyt *c* redox potentials associated with different conformational states. Long lines show midpoint potentials. The bold long lines are the native (+50 mV) and his–his or his–water heme conformational states. The short lines show positions of oxidation waves as examples.

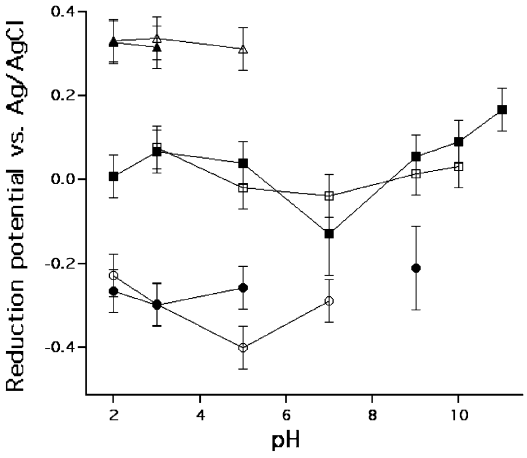

Fig. 6. The positions of redox midpoint potentials as observed in CV scans as a function of pH. Uncertainties are based on the uncertainty in locating both the reduction and oxidation waves for a given redox wave in the CV scans at different scan rates. Empty and filled circles, triangles and squares denote redox midpoint potentials in the absence and presence of phosphate, respectively.

pH in Fig. 6. The high potential peak is characteristic of low pH environments, consistent with its attribution to a positively charged heme environment in Cyt *c* [56]. This peak persists up to pH 5 in the absence of phosphate but only to pH 3 in the presence of phosphate, suggesting a Cyt *c* stabilizing effect of phosphate. The native conformational state is observed at both lower and higher pH in the presence of phosphate than in its absence, also suggesting a stabilizing influence of phosphate.

The unfolded histidine–histidine or histidine–water conformational state at negative redox potential is more problematic. This peak is evident without phosphate but not with phosphate at pH 7, but the opposite is true at pH 9. At pH 7 in particular the peaks become very broad and difficult to distinguish from the native conformational redox waves, and it is possible that these two peaks overlap at pH 7 in the presence of phosphate. We have included in Fig. 6 only those redox waves for which both a reduction and oxidation wave could be identified. At pH 10 and 11, an oxidation wave was observed at −220 and −330 mV, respectively, without a corresponding reduction wave. This was also observed at high pH in control CV scans without Cyt *c*, and we cannot therefore attribute them to Cyt *c* and they are not plotted in Fig. 6. However, we cannot rule out overlap between an unfolded Cyt *c* response and the control response.

A (6cLS) species of Cyt *c* was observed after adsorption at negative potentials (<−0.2 V vs SCE) on an Ag electrode, whereas adsorption at positive potentials stabilized a second conformer characterized by a mixture of 5cHS and 6cLS configurations [50]. This is qualitatively consistent with our results because it shows that formation of different conformational states can occur because of changing surface electrostatics. The 5cHS reduction potential [50] is comparable to our negative-potential peak in Figs. 5 and 6, which is most prevalent at pH < pzc of hematite, again consistent with [50].

Overall, the presence of phosphate does not dramatically increase the currents observed in CV scans, suggesting either that phosphate does not play a strong role in favorably orienting Cyt *c* on hematite electrode surfaces for electron transfer or that Cyt *c* undergoes conformation changes in the adsorbed state that obviate any need for orientation. Also, the Schottky barrier at the electrode surface may be the main current-limiting factor. Phosphate appears to have a stabilizing influence such that native-state redox waves are observed at both higher and lower pH than in its absence. The factors affecting changes in redox potential include solvent exposure of the heme, the tertiary structure of the protein, the spin state of Fe in heme and its axial ligands [50]. While the optical absorption spectra are sensitive to conformation changes in the heme macrocycle only, the reduction potentials also probe changes in tertiary structure of the protein. The fact that we observe native-state redox potentials up to pH 11 is interesting relative to the observation that native-state histidine–methionine heme coordination is lost in solution (in optical absorption spectra) above pH 7. This suggests that the electrode surface may have a stabilizing effect on Cyt *c*.

The effect of adsorption may be rather complex. Tie and Calonder [60] show that the rate of Cyt *c* adsorption to $Si_{0.75}Ti_{0.25}O_2$ surfaces, at a given coverage of previously adsorbed Cyt *c*, depends on how long the previous Cyt *c* coverage has existed. This implies substantial conformation change on an oxide, over time, by adsorbed Cyt *c*. This is consistent with other findings [61] showing that Cyt *c* blocks carbon electrodes through conformation change such that native-state protein becomes difficult to observe electrochemically. We suggest that our hematite electrodes become coated with conformationally altered protein, and that this protein coating, perhaps synergistically with phosphate, helps subsequent Cyt *c* to retain or regain native characteristics when it interacts with the (protein-coated) hematite electrode. It should be noted that a monolayer of adsorbed Cyt *c* (assuming hexagonal close packing) would support about 200 nA of peak current given our electrode sizes (at 20 mV s^{-1} scan rate); this is comparable to or smaller

than the currents we observe experimentally. Therefore, it is reasonable to conclude that the currents we observe can be attributed to a combination of oxidation–reduction of an adsorbed protein layer as well as oxidation–reduction of dissolved protein diffusing to the (protein-coated) electrode surface. We conducted scan rate dependence studies in an attempt to distinguish currents due to adsorbed vs dissolved protein, but the frequency-dependent capacitive currents resulting from charging and discharging the semiconductor space charge layer [55] complicate the interpretation (data not shown).

3.4. Supernatant solutions without phosphate

The absorption spectra of supernatant solutions resulting from Cyt *c* adsorption experiments (after centrifugal removal of hematite particles) show essentially similar Soret, Q, and charge transfer band positions between pH 2 and 7 as in solutions never exposed to hematite (Fig. 7). However, between pH 7 and 12, the Soret band (409 to 412 nm) was consistently red-shifted, indicating destabilization of the heme macrocycle (Fig. 7). The 695 nm charge transfer band is missing, indicating loss of Fe–S ligation (Fig. 7c). The Q bands change from a broad peak at 530 nm and a weak shoulder at 550 nm to showing a broad peak at 522 nm and another peak at 548 nm (Fig. 7b).

Following from the concept of microscopic reversibility, the Cyt *c* supernatant solutions can be considered to be a mixture of Cyt *c* that has never been sorbed to hematite together with Cyt *c* that has been sorbed and then desorbed. Cyt *c* that has been sorbed and then desorbed may misfold upon desorption and thus not retain native conformation once redissolved in supernatant solutions. Because relatively small amounts of Cyt *c* sorb to hematite between pH 2 and 7 and because desorption is relatively slow [60], the spectra for supernatant solutions are largely representative of Cyt *c* in solution that has never been sorbed to the surface. Between pH 8 and 10 however, the spectra for supernatant solutions show evidence for destabilization of the heme macrocycle and replacement of methionine by another ligand (possibly water or a histidine; [29]) while Fe is maintained in the low spin state. Electrochemically, we nevertheless observe a native-state redox wave, again suggesting that the surface stabilizes the native state as discussed above.

3.5. Supernatant solutions with phosphate

The Soret band of supernatant solutions for Cyt *c* co-sorbed with 0.01 M phosphate on hematite surfaces are shown in Fig. 8. The spectra show either native Soret and Q band positions or are slightly (2 nm) blue shifted, the 695 nm band is present from pH 3–8 but absent at all other pH values (Fig. 7c), and up to pH 10 the spectra are similar to those for solutions (of Cyt *c* dissolved with phosphate) that were never exposed to hematite. This may be because (a) there is little or no sorption-induced conformation change in the presence of phosphate because phosphate acts as a linker molecule allowing Cyt *c* to maintain solution-like conformation on hematite surfaces, or (b) phosphate causes Cyt *c* to aggregate, and if the aggregate sorbs many of the Cyt *c* molecules may not come into contact with the surface

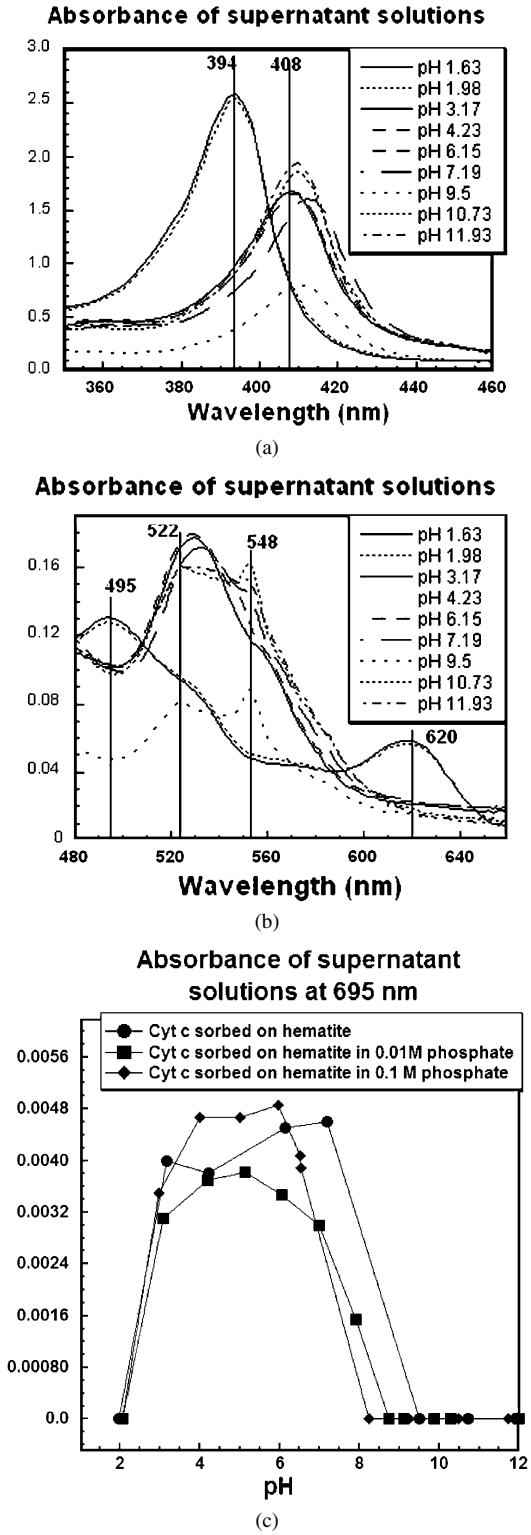

Fig. 7. Optical absorbance of supernatant solutions resulting from Cyt *c* sorption experiments with hematite. Because the concentration of Cyt *c* in supernatant solutions was based on molar absorptivity in solution, molar absorptivity of supernatant solutions could not be independently compared: (a) Soret band; (b) Q bands; (c) absorbance at 695 nm in solutions with different phosphate concentrations.

and may thus maintain a conformation state characteristic of Cyt *c* interaction with phosphate, or (c) Cyt *c* changes conformation on sorption, but phosphate aids refolding of Cyt *c* when

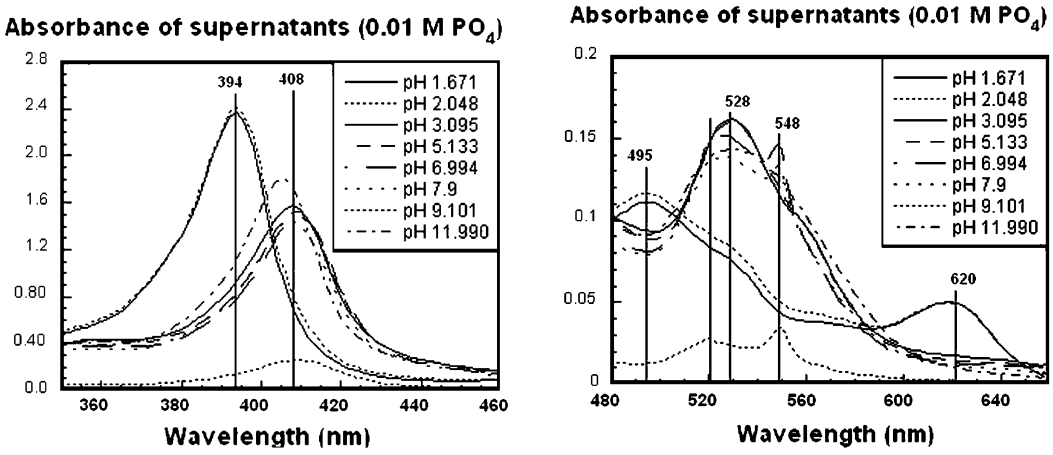

Fig. 8. Optical absorbance of supernatant solutions of Cyt *c* co-sorbed with 0.01 M phosphate on hematite. (a) Soret band; (b) Q bands.

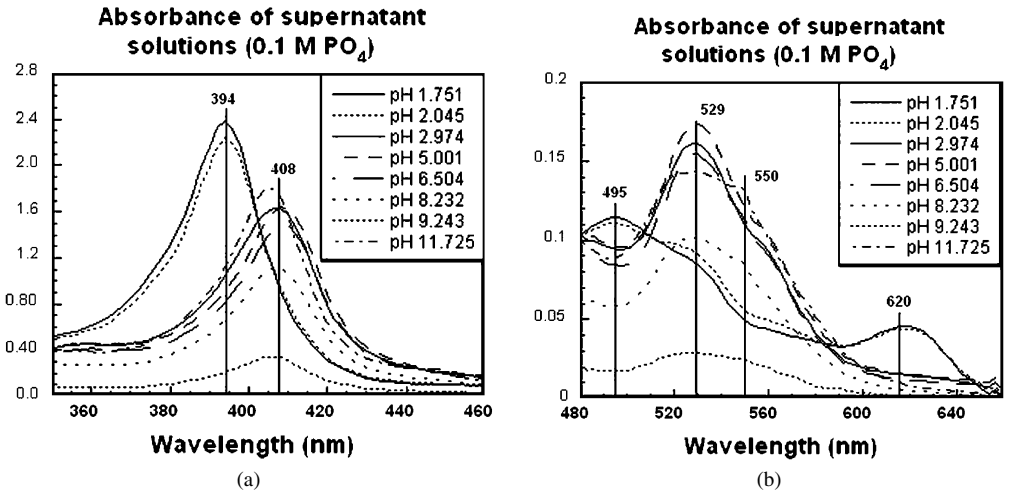

Fig. 9. Optical absorbance of supernatant solutions of Cyt *c* co-sorbed with 0.1 M phosphate on hematite. (a) Soret band; (b) Q bands.

it desorbs. Further evidence is available (see below) from AFM imaging.

The Soret and Q bands of supernatant solutions for Cyt *c* co-sorbed with 0.1 M phosphate on hematite surfaces are found in Fig. 9 and show either native or slightly (2 nm) blue shifted Soret band positions, similar to the trends observed in Cyt *c* solutions dissolved in 0.01 M phosphate. The 695 nm band is also present from pH 3–7 (but not up to 8) in Cyt *c* co-sorbed with 0.1 M phosphate on hematite but absent at all other pH values (Fig. 7c). Only a broadened Q band at ∼530 nm (see also Fig. 5b) is observed, unlike the splitting of the Q band observed in Cyt *c* solutions and in supernatant from Cyt *c* alone and co-sorbed with 0.01 M phosphate on hematite. UV–visible absorption spectra for Cyt *c* in pH 7.5 phosphate buffer sorbed on a quartz slab optical waveguide show a Soret band at 405 nm and Q band at 530 nm of intensity ratio 2.5 [62] instead of 10 observed in solution, providing evidence of conformation change in the heme macrocycle. Our results suggest that increasing phosphate concentration in the supernatant solutions would aid in neutralizing the effect of sorption induced conformation change in the heme macrocycle observed by Kato et al. [62].

3.6. AFM observations

A sequence of contact AFM images of a hematite surface in 0.1 M NH_4PO_4 (pH 8) with 2.5×10^{-5} M Cyt *c* is found in Fig. 10. Fig. 10a shows a high force scan (contact force ∼200 nN) that cleared the surface of adsorbed Cyt *c* and thus shows the underlying terraces and monolayer and bilayer steps. Upon reducing the contact force (to ∼2 nN), Cyt *c* rapidly coats the surface of hematite (Fig. 10b). After waiting about 5 more min. and then scanning a 1×1 μm^2 area at high force, a scan field is created in which Cyt *c* has again been displaced from the surface and which is visible in the larger image (Fig. 10c) but which begins to fill in during the low force scan used to image it. These adsorption rates are consistent with the findings of Calonder et al. [63], who studied the kinetics of Cyt *c* sorption to $Si_{0.75}Ti_{0.25}O_2$ surfaces and found that rapid initial adsorption led to formation of about 0.5 monolayer in 1 min. At pH 8 in Fig. 1, we should expect roughly 2 monolayers of coverage given 10^{-4} M starting Cyt *c* concentration. In Fig. 10c, the depth of the scan field is roughly 3 nm in places that are not filled in with resorbed protein, although this estimate has roughly 2 nm error because of both noise and local topograph-

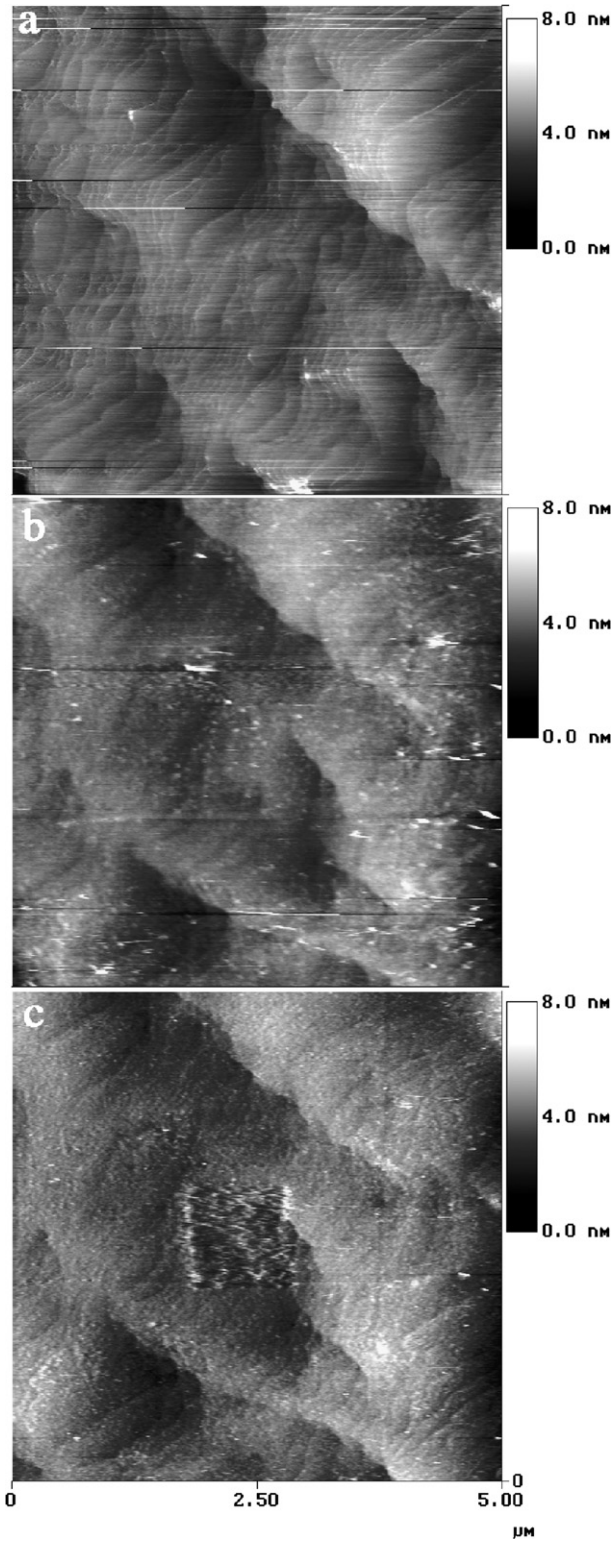

Fig. 10. Contact mode AFM images of hematite surface exposed to 0.1 M NH_4PO_4 and 0.3 mg mL^{-1} Cyt *c* in contact mode; (a) at high contact force (∼200 nN) showing steps and terraces; (b) upon reducing the contact force (∼2 nN), Cyt *c* rapidly coats the surface (scan completed approximately 1 min after (a); (c) 1×1 μm^2 area scanned at high force creating a scan field in which Cyt *c* has been displaced from the surface.

ical variation. This coverage is, however, comparable to the results reported in Fig. 1 (the starting Cyt *c* concentration is 4 times lower than for Fig. 1, but the solution-to-surface area ratio is higher). The adsorbed particles have an apparent diameter of 20 to 30 nm laterally, with some particles ranging up to 60 nm. We agree with the interpretation of Boussad et al. [19], who observed Cyt *c* co-sorbed with phosphate as bumps 20–30 nm wide and 3–5 nm high (consistent with a native molecular diameter of 3.4 nm) on a graphite electrode. Their images were interpreted as Cyt *c* in the native state, with expanded lateral dimensions caused tip broadening (i.e., tip radius of curvature is greater than that of the observed molecule). We suspect that the particles larger than about 20 nm, however, are small aggregates of more than one Cyt *c* molecule.

Fig. 11 shows a hematite surface imaged in situ at pH 8 before (Fig. 11a) and after addition of 10^{-4} M Cyt *c* solution with 0.01 M phosphate (Fig. 11b). Again, adsorption is relatively rapid. The scan field cleared of protein with high contact force is only 1–2 nm deep, however (compared to neighboring protein-coated surface but excluding the piled-up protein on the left and lower sides of the scan field), suggesting that the protein is either more easily deformed by the AFM tip pressure in this case, or has undergone a conformation change. As a test of the effect of AFM tip pressure, we used a high force scan to clear another area of protein, and then imaged the area in AC (oscillating cantilever) mode. A resulting image is found in Fig. 11c; again, bumps 1–2 nm high and 20–30 nm wide are apparent, along with some bumps that are up to 60 nm wide. Although the images are less "streaky" in AC mode, the vertical molecular dimensions have not changed. This suggests that the sorbed Cyt *c* has undergone a conformation change upon sorption, resulting in a reduced vertical dimension. However, we cannot entirely rule out molecular deformation by the AFM tip in AC mode. Again, the larger particles are probably aggregates of Cyt *c* molecules rather than single molecules.

The electrochemical data show evidence for an unfolded Cyt *c* conformation at pH 9 in the presence of phosphate, but not at pH 7. We speculate that the formation of aggregates helps to hold some of the Cyt *c* in each aggregate in a native conformation, and that solution Cyt *c* molecules that interact with the surface to exchange electrons is stabilized by the protein-coated surface. Some protein in direct contact with the surface, probably undergoes conformation change. Cyt *c* aggregation in solution is dependent on the concentration of the background electrolyte and reflected in the broadening of the Soret band [49,65]. It has been previously observed in the presence of hexametaphosphate [49]. However, in our studies the low ionic strength of 0.01 M was not conducive to protein aggregation as evidenced by nearly constant full width at half maximum height (fwhm) for our Soret bands for solution Hcc at different pH.

4. Conclusions

The pH dependence of Cyt *c* sorption to hematite surfaces in the presence of phosphate is consistent with electrostatic attraction. The occurrence of multilayer adsorption, and our AFM observations, suggest however that Cyt *c* forms aggregate particles as the pH approaches the isoelectric point of the protein. In solution without phosphate, our optical absorption data are in agreement with previous studies in showing Cyt *c* unfold-

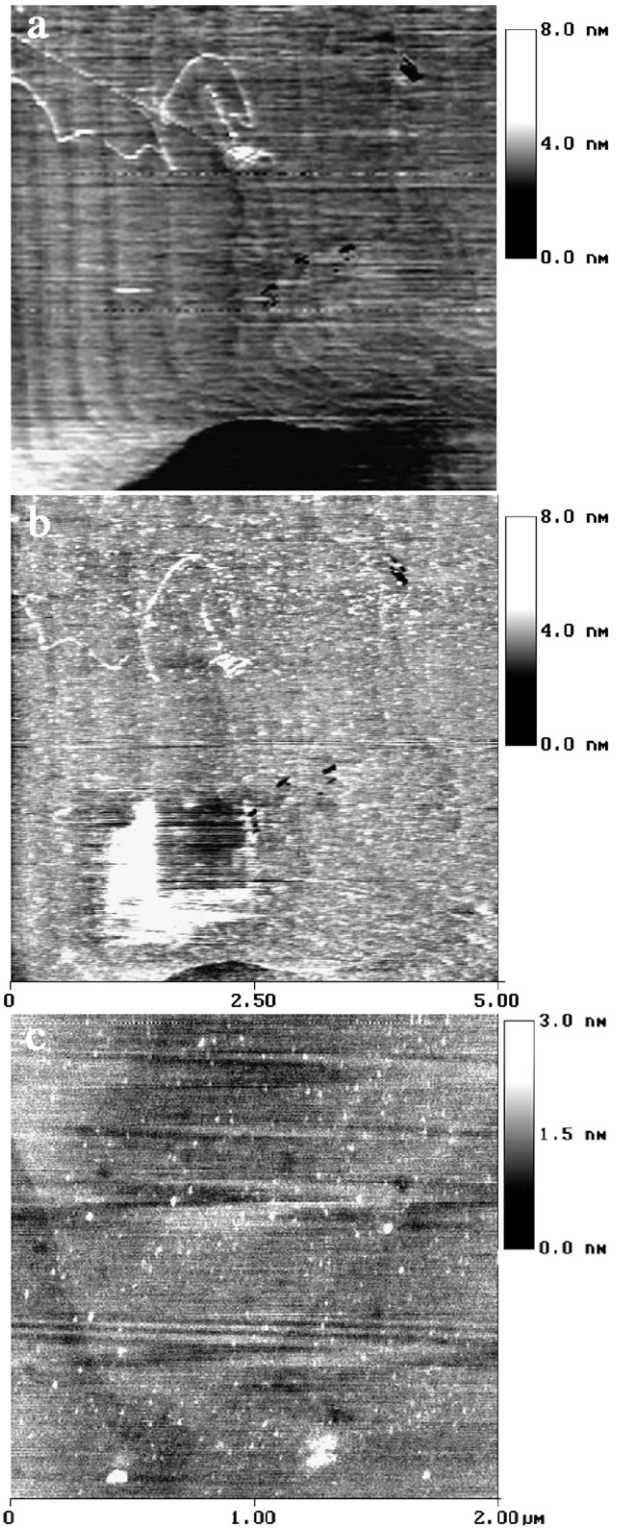

Fig. 11. AFM images of 0.3 mg mL^{-1} Cyt *c* co-sorbed with 0.01 M phosphate at near neutral pH: (a) in solution prior to introduction of Cyt *c*; (b) same surface after introduction of Cyt *c*; (c) an AC-mode image of Cyt *c* molecules on a hematite surface after a high-force contact AFM scan (see text).

ing and formation of a 6cHS state at pH < 3, but the loss of methionine coordination of the heme Fe occurs at pH > 7. In the presence of phosphate, methionine coordination is retained up to pH 10, suggesting that phosphate stabilizes the protein against unfolding. At low pH, electrochemical evidence using hematite electrodes suggests that a native conformational state occurs down to pH 3 and up to pH 10 in the absence of phosphate, and that this range is extended to pH 2 and 11 in the presence of phosphate. At low pH, other conformationally altered forms of Cyt *c* occur as well, perhaps reflecting conformational equilibrium between native and unfolded states (e.g., Yeh and Rousseau [64]). Our results suggest that Cyt *c* that initially adsorbs to the hematite surface may undergo a conformation change and coat the surface with unfolded protein such that subsequent protein that interacts with the (protein-coated) surface is more likely to retain a native conformational state. Phosphate appears also to help stabilize the native conformational state. We propose that the redox currents that we observe with voltammetry indicate electron transfer from the hematite electrode to both unfolded protein heme groups near the electrode surface, as well as to native-state protein (with some conformationally altered protein at low pH) in the near-surface solution. Aggregates likely help to preserve Cyt *c* in native conformation.

Acknowledgments

The authors gratefully acknowledge support from the National Science Foundation, EAR-987530 and EAR-0434019; any opinions, findings, and conclusions or recommendations expressed in this material are those of the authors and do not necessarily reflect those of the National Science Foundation.

References

[1] P. Yeh, T. Kuwana, Chem. Lett. 1977 (1977) 1145.
[2] E. Lojou, P. Bianco, M. Bruschi, J. Electroanalyt. Chem. 452 (1998) 167.
[3] C.E. Castro, R.S. Wade, N.O. Belser, Biochemistry 24 (1985) 204.
[4] R. Shanker, W.M. Atkins, Biotechnol. Progr. 12 (1996) 474.
[5] M. Wirtz, J. Klucik, M. Rivera, J. Am. Chem. Soc. 122 (2000) 1047.
[6] L. Gorton, A. Lindgren, T. Larsson, F.D. Munteanu, T. Ruzzas, I. Gazaryan, Anal. Chim. Acta 400 (1999) 91.
[7] K. Kano, T. Ikeda, Anal. Sci. 16 (2000) 1013.
[8] V. Fridman, U. Wollenberger, V. Bogdanovskaya, F. Lisdat, T. Ruzgas, A. Lindgren, L. Gorton, F.W. Scheller, Biochem. Soc. Trans. 28 (2000) 63.
[9] D.R. Lovley, E.J.P. Philips, Appl. Environ. Microbiol. 60 (1994) 726.
[10] J.R. Lloyd, V.A. Sole, C.V.G. Van Praagh, D.R. Lovley, Appl. Environ. Microbiol. 66 (2000) 3743.
[11] D.E. Holmes, K.T. Finveran, R.A. O'Neil, D.R. Lovley, Appl. Environ. Microbiol. 68 (2002) 2300.
[12] C. Liu, Y.A. Gorby, J.M. Zachara, J.K. Fredrickson, C.F. Brown, Biotechnol. Bioeng. 80 (2002) 637.
[13] D.E. Cummings, D.L. Snoeyenbos-West, D.T. New, A.M. Niggemeyer, D.R. Lovley, L.A. Achenbach, R.F. Rosenzweig, Microb. Ecol. 46 (2003) 257.
[14] E. Topoglidis, C.J. Campbell, E. Palomares, J.R. Durrant, Chem. Comm. 2002 (2002) 1518.
[15] R. Das, P.J. Kiley, M. Segal, J. Norville, A.A. Yu, L. Wang, S.A. Trammell, L.E. Reddick, R. Kumar, F. Stellacci, N. Lebedev, J. Schnur, B.D. Bruce, S. Zhang, M. Baldo, Nano Lett. 4 (2004) 1079.
[16] D. Cao, P. He, N. Hu, Analyst 128 (2003) 1268.
[17] M.J. Eddowes, H.A.O. Hill, J. Chem. Soc. Chem. Comm. 1977 (1977) 771.
[18] S. Boussaad, L. Dziri, R. Arechabaleta, N.J. Tao, R.M. Leblanc, Langmuir 14 (1998) 6215.

[19] S. Boussaad, N.J. Tao, R. Arechabaleta, Chem. Phys. Lett. 280 (1997) 397.
[20] R.T. Shuey, Semiconducting Ore Minerals, Elsevier, Amsterdam, 1975.
[21] M. Anderman, J.H. Kennedy, in: H.O. Finklea (Ed.), Semiconductor Electrodes, Elsevier, Amsterdam, 1988, p. 147.
[22] C.M. Eggleston, A.G. Stack, K.M. Rosso, S.R. Higgins, A.M. Bice, S.W. Boese, R.D. Pribyl, J.J. Nichols, Geochim. Cosmochim. Acta 67 (2003) 985.
[23] A. Brack, The Molecular Origins of Life: Assembling Pieces of the Puzzle, Cambridge Univ. Press, Cambridge, UK, 1998.
[24] S.J. Field, P.S. Dobbin, M.R. Cheesman, N.J. Watmough, A.J. Thomson, D.J. Richardson, J. Biol. Chem. 275 (2000) 8515.
[25] T.S. Magnuson, N. Isoyama, A.L. Hodges-Myerson, G. Davidson, M.J. Maroney, G.G. Geesey, D.R. Lovley, Biochem. J. 359 (2001) 147.
[26] C.R. Myers, J.M. Myers, Lett. Appl. Microbiol. 37 (2003) 254.
[27] L. Shi, L. Jiann-Trzwo, L.M. Markillie, T.C. Squier, B.S. Hooker, BioTechniques 38 (2005) 297.
[28] D. Keilin, Proc. R. Soc. London B Biol. Sci. 98 (1925) 312.
[29] H. Theorell, A. Akesson, J. Am. Chem. Soc. 63 (1941) 1804.
[30] H. Theorell, A. Akesson, J. Am. Chem. Soc. 63 (1941) 1812.
[31] H. Theorell, A. Akesson, J. Am. Chem. Soc. 63 (1941) 1818.
[32] H. Theorell, A. Akesson, J. Am. Chem. Soc. 63 (1941) 1820.
[33] Y.G. Thomas, R.A. Goldbeck, D.S. Kliger, Biopolymers 57 (2000) 29.
[34] S. Oellerich, H. Wackerbarth, P. Hildebrandt, J. Phys. Chem. B 106 (2002) 6566.
[35] N. Khare, C.M. Eggleston, D.M. Lovelace, Clays Clay Min. 53 (2005) 564.
[36] T. Sugimoto, A. Muramatsu, K. Sakata, D. Shindo, J. Colloid Interface Sci. 158 (1992) 420.
[37] N. Khare, D. Hesterberg, S. Beauchemin, S.L. Wang, Soil Sci. Soc. Am. J. 68 (2004) 460.
[38] T.J.T. Pinheiro, Biochimie 76 (1994) 489.
[39] L.A. Dick, A.J. Haes, R.P. Van Duyne, J. Phys. Chem. 104 (2000) 11752.
[40] L. Stryer, Biochemistry, fourth ed., Freeman, New York, 1995.
[41] M.R. Gunner, A. Nicholls, B. Honig, J. Phys. Chem. 100 (1996) 4277.
[42] Y. Sallez, P. Bianco, E. Lojou, J. Electroanalyt. Chem. (2000) 37.
[43] F. Boffi, S. Bonincontro, A. Cinelli, C. Castellano, A. Francesco, S. Della Longa, M. Girasole, G. Onori, Biophys. J. 80 (2001) 1473.
[44] W. Stumm, J.J. Morgan, Aquatic Chemistry, third ed., Wiley, New York, 1996.
[45] G.W. Pettigrew, G.R. Moore, Cytochromes *c*: Biological Aspects, Springer-Verlag, New York, 1987.
[46] M. Schudel, S.H. Behrens, H. Holthoff, R. Kretzschmar, M. Borkovec, J. Colloid Interface Sci. 196 (1997) 241.
[47] B.L. Neal, D. Asthagiri, O.D. Velev, A.M. Lenhoff, E.W. Kaler, J. Cryst. Growth 196 (1999) 377.
[48] A.B. Anderson, D.R. Robertson, Biophys. J. 68 (1995) 2091.
[49] D. Whitford, D.W. Concar, R.J.P. Williams, Eur. J. Biochem. 199 (1991) 561.
[50] P. Hildebrandt, M. Stockburger, Biochemistry 28 (1989) 6710.
[51] P. Hildebrandt, M. Stockburger, Biochemistry 28 (1989) 6722.
[52] M.T. Wilson, C. Greenwood, in: R.A. Scott, A.G. Mauk (Eds.), Cytochrome-c: A Multidisciplinary Approach, University Science Books, Sausalito, 1996, p. 611.
[53] Q. Xu, T.A. Kiederling, Biopolymers 73 (2004) 716.
[54] S.B. Mendes, L. Li, J.J. Burke, Langmuir 12 (1996) 3374.
[55] C. Sanchez, K.D. Sieber, G.A. Somorjai, J. Electroanalyt. Chem. 252 (1988) 269.
[56] X. Chen, R. Ferrigno, J. Yang, G.M. Whitesides, Langmuir 18 (2002) 7009.
[57] L.J.C. Jeuken, Biochim. Biophys. Acta 1604 (2003) 67.
[58] R.O. Louro, E.C. de Waal, M. Ubbink, D.L. Turner, FEBS Lett. 510 (2002) 185.
[59] F.A. Tezcan, J.R. Winkler, H.B. Gray, J. Am. Chem. Soc. 120 (1998) 13383.
[60] Y. Tie, C. Calonder, P.R. Van Tassel, J. Colloid Interface Sci. 268 (2003) 1.
[61] H.A.O. Hill, N.I. Hunt, A.M. Bond, J. Electroanalyt. Chem. 436 (1997) 17.
[62] K. Kato, A. Takatsu, N. Matsuda, Chem. Lett. 139 (1999) 31.
[63] C. Calonder, Y. Tie, P.R. Van Tassel, Proc. Natl. Acad. Sci. USA 98 (2001) 10664.
[64] S.R. Yeh, D.L. Rousseau, J. Biol. Chem. 274 (1999) 17853.
[65] X. Peng, J. Huang, L. Ji, Chin. Sci. Bull. 45 (2000) 418.